Preparation of Sonocatalyst Fe₂O₃/ZnO using Sol-gel/precipitation Method: Characterization and Removal of Acid Orange 7 in Aqueous Solution

Nur Fadzeelah A. K.[1] and Nor Aimi Abdul Wahab[2]

[1]*Faculty of Chemical Engineering, UiTM Cawangan Pulau Pinang, 13500 Permatang Pauh, Pulau Pinang, Malaysia*
[2]*Department of Applied Science, UiTM Cawangan Pulau Pinang, 13500 Permatang Pauh, Pulau Pinang, Malaysia*
Corresponding author: nurfadzeelah122@ppinang.uitm.edu.my

ARTICLE HISTORY	ABSTRACT

Fe₂O₃/ZnO composite catalyst was synthesized using a sol-gel/precipitation method. The synthesized samples were characterized by X-ray diffraction (XRD), scanning elctron microscope (SEM) with energy dispersive X-tray spectroscopy (EDX) and Brunauer−Emmet−Teller (BET) method. The feasibility of Fe₂O₃/ZnO composite catalyst on the removal of Acid Orange 7 (AO7) solution was examined under an ultrasonic irradiation. The removal percentage of AO7 solution was monitored by UV-vis spectrophotometer. The characterization results exhibited that the Fe₂O₃/ZnO composite catalyst was successfully prepared using the sol-gel/precipitation method. The loading of Fe₂O₃ particles on the surface of ZnO particles resulted in high surface area compared to ZnO catalyst. Performance wise, the highest removal percentage of AO7 solution for sonocatalytic activity (at 120 min) showed only 8.05% and 9.12% for ZnO catalyst and Fe₂O₃/ZnO composite catalyst, respectively. Thus, the poor removal of AO7 solution in sonocatalytic experiment using this composite catalyst indicating this catalyst is not a good potential as sonocatalyst in treatment of azo dyes. In addition, this study has revealed that Fe₂O₃/ZnO composite catalyst was superior to the adsorption activity in removing of AO7 from aqueous solution due to adsorption ability of Fe₂O₃.

Keywords: *Fe₂O₃/ZnO; AO7; sol-gel/precipitation; composite catalyst; sonocatalytic degradation*

1. INTRODUCTION

Industrial wastewater has been considered as one of the main contributors to water pollution. The wastewater of textile, cosmetic, plastic food and pharmaceuticals industries contain various organic dye and pigments, which can cause environmental hazards. Seventy percent of the dye used in the industry consist of azo dye [1]. Azo dyes are characterized by the existence of one or more azo bonds (-N=N-), attached to one or more aromatic structures, which impart their stability. These azo dyes are very toxic to living organism, carcinogenic in nature, mutagenic and very difficult to degrade biologically due to its complex structure and stability [2]. Discharge of these azo dyes can interfere with the transmission of sunlight into streams and therefore reducing photosynthetic activity. Due to an adverse effect on health and

environment, there is an urgent need for the removal of these azo dyes from wastewater. Advance oxidation processes (AOPs) have been receiving a widely attention as it is considered as an efficient method for oxidation of many resistant organic contaminants in the environment [3]. Among these AOPs, ultrasound based sonochemical process has been considered as a possible method for water treatment due to its high efficiency and easy operation [4]. During this process, ultrasound waves lead to a quick growth and collapse of microbubble within the solution, resulting in extremely high temperature and pressure in the bubbles. High temperature created near the cavitation bubbles cause a thermal dissociation of water and generates into hydrogen and hydroxyl radicals as a strong oxidant for non-selective oxidation of organic pollutant [4].

However the limitation of this method is that it needs high energy and is time consuming at a low degradation rate [5]. To overcome such limitations, the combination of catalyst with sonolysis (sonocatalysis process) has been applied to enhance the degradation efficiency of various pollutants. The enhancement in degradation is caused by the collaborative effect of sonolysis with solid catalyst which provides additional active site for the nucleation of bubbles. The solid particles also increase the mass transfer of pollutant between the liquid and the surface of the catalyst [6]. ZnO has been widely used in the sonocatalytic process for the degradation of organic pollutant due to its unique physical and chemical characteristic. ZnO catalyst is commonly synthesized using sol-gel technique due to its low cost, simplicity and low temperature requirement which allow for the finer control of the product's chemical composition. Properties of ZnO including high exciton binding energy (60 meV), wide band gap (3.37 eV) and high UV absorption potential making it a suitable choice as the sonocatalyst [7]. However, pure ZnO has fast recombination of the generated electron whole pairs which affected the catalytic activity. In the study conducted by Wang et al. [8], they found that the prepared composite of TiO_2/ZnO powder exhibited high sonocatalytic activity and concluded that the composite catalyst was a more preferable sonocatalyst compared to pure TiO_2 and ZnO catalyst.

Precipitation method has been adopted for the preparation of composite acknowledging its numerous advantages as it does not require complicated equipment and extreme experimental condition. It can also produce high quality product with uniform powders and particle size [9]. Besides, Ce-doped ZnO nanoparticles prepared using this method, exhibited a narrowed band gap and higher catalytic performance of methyl orange than an undoped one [10]. In addition, another study on SrF_2 nanopowders activated by Nd^{3+} via precipitation method shows good sinterability and can be fabricated to transparent ceramics with a transmittance of about 80% at 1060 nm by vacuum [11].

In this study, sol-gel/precipitation method was employed to prepare Fe_2O_3/ZnO composite catalyst. The detail characterizations of the as-prepared composite catalyst were discussed and Acid Orange 7 (AO7) was used as a model of azo dye to investigate the sonocatalytic degradation activity of this composite catalyst. The aim was to study the catalytic potential of Fe_2O_3/ZnO composite catalyst in the removal of AO7 solution.

2. MATERIALS AND METHODS

2.1 Materials

Zinc Acetate Dihydrate ($Zn(O_2CCH_3)_2(H_2O)_2$) (98% purity), Citric Acid ($C_6H_8O_7$) (98% purity), Iron(III) Nitrate Nonahydrate ($Fe(NO_3)_3.9H_2O$) (99.9% purity) and urea (CH_4N_2O) were used as received without any purification. Acid Orange 7 (AO7) ($C_{16}H_{11}N_2NaO_4S$) was purchased from Sigma Aldrich (M) and used as the model pollutant in this study. Distilled water was used throughout this study for catalyst preparation and AO7 dilution.

2.2 Preparation of ZnO and Fe₂O₃/ZnO

Zinc oxide was prepared using sol-gel method [12] with zinc acetate dehydrate and citric acid as the starting materials. The dehydrated zinc acetate (1.23 g) and citric acid (5.50 g) were dissolved in 250 mL distilled water. The solution was vigorously stirred for one hour where a clear and homogenous solution was formed. Then, the solution was dried at 100°C for 12 hours in an oven until it formed a dried gel. The dried gels were then sieved to produce fine powders and were calcined in the furnace for two hours at 300°C. The powders were then subjected to second calcination at 500°C for two hours before the final ZnO powder was obtained.

The composite catalyst of Fe_2O_3/ZnO was prepared by using precipitation method which was adapted from [13]. A 0.4 g of the prepared ZnO, 0.6 g $Fe(NO_3)_3.9H_2O$ and 0.6 g CH_4N_2O were mixed in 100 mL distilled water and was vigorously stirred for one hour at 100°C. Then, the solution was allowed to cool down at room temperature for one hour until the required precipitate was formed. Afterwards, the remaining aqueous solution was filtered out and washed multiple times with distilled water–ethanol mixture to further purify the Fe_2O_3/ZnO particles. Subsequently, the sample was dried overnight at 120°C before calcined at 600°C for one hour. This final material, Fe_2O_3/ZnO can be described as a composite catalyst with a ratio of 1:2. The preparation steps for both catalysts are simplified in Figure 1.

2.3 Characterization of Fe₂O₃/ZnO

Surface morphology and elemental composition of the ZnO and Fe_2O_3/ZnO catalysts were investigated using Hitachi TM3030 scanning electron microscopy (SEM) at accelerating voltage of 15 kV. The purity of elemental analysis of the samples was obtained by energy dispersive X-tray spectroscopy (EDX) with the same instrument.

XRD analysis of the catalysts was carried out using X-ray diffractometer (Bruker D8 Advance, Germany) with Cu Kα radiation source (λ = 1.540600 Å), which operated at accelerating voltage of 40 kV and emission current of 40 mA. The samples were scanned from 10° to 70° at step size of 0.020°. The diffraction peaks were assigned to the corresponding crystalline phases by comparison with the International Centre for Diffraction Data (ICDD) database. The average crystallite size was estimated by application of Scherrer Equation: $D_{avg} = 0.94\lambda/\beta \cos\theta$.
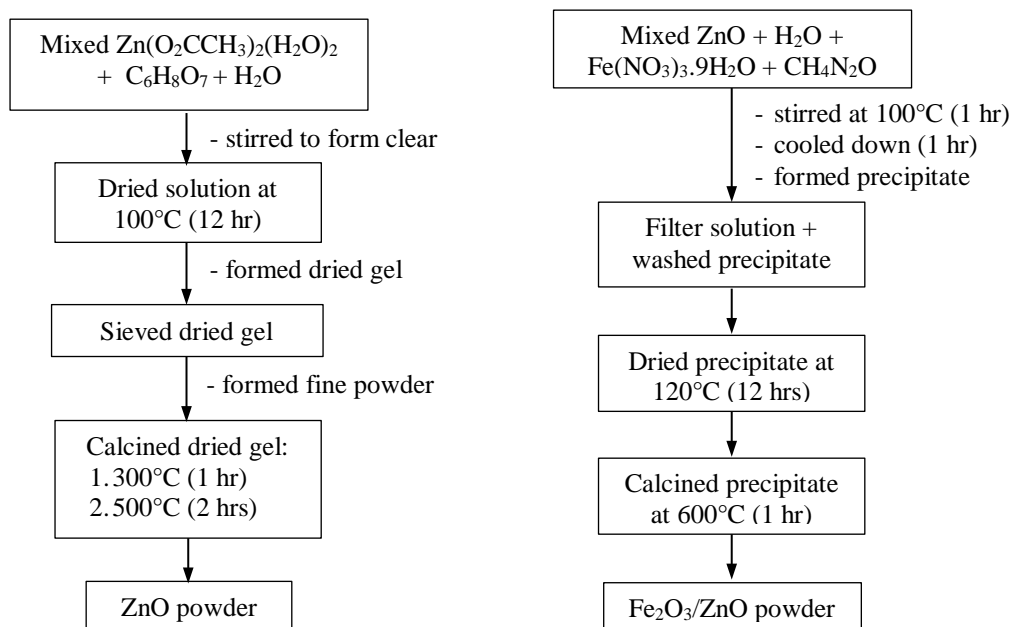
Figure 1: Flowchart of catalyst preparation

2.3 Characterization of ZnO and Fe₂O₃/ZnO

Surface morphology and elemental composition of the ZnO and Fe_2O_3/ZnO catalysts were investigated using Hitachi TM3030 scanning electron microscopy (SEM) at accelerating voltage of 15 kV. The purity of elemental analysis of the samples was obtained by energy dispersive X-tray spectroscopy (EDX) with the same instrument.

XRD analysis of the catalysts was carried out using X-ray diffractometer (Bruker D8 Advance, Germany) with Cu Kα radiation source (λ = 1.540600 Å), which operated at accelerating voltage of 40 kV and emission current of 40 mA. The samples were scanned from 10° to 70° at step size of 0.020°. The diffraction peaks were assigned to the corresponding crystalline phases by comparison with the International Centre for Diffraction Data (ICDD) database. The average crystallite size was estimated by application of Scherrer Equation: $D_{avg} = 0.94\lambda/\beta \cos\theta$.

Nitrogen physisorption measurements were conducted using Micromeritics instrument model ASAP 2020 at -195.820°C. The samples (0.1279 g for ZnO) and (0.1025 g for Fe_2O_3/ZnO) were degassed under vacuum at 300°C for four hours. The surface area was calculated using the standard Brunauer–Emmet–Teller (BET) method while the pore volume and size were calculated by Barret-Joyner-Halenda (BJH) for mesopores analysis.

2.4 Experiment Set-Up and Sonocatalytic Degradation Procedure

A beaker was filled with 100 mL of AO7 solution (20 mg/L) and appropriate catalyst dosage of 1 g/L. All experiments were performed at natural pH (~6.20) of AO7 solution and the pH of this solution was left uncontrolled throughout the experiments. In a typical heterogeneous

catalytic experiment, the suspended solution was placed in the dark condition for 30 minutes under magnetic stirring to establish adsorption–desorption equilibrium of the dye compound on the catalyst surface. After the adsorption state, the concentration of AO7 solution was reset as initial concentration, C_i, for the sonocatalytic degradation experiment.

Then, the sonocatalytic degradation experiment was carried out further in an open of glass vessel (300 mL beaker) for 120 minutes under ultrasonic irradiation. An ultrasonic bath type (Elmasonic S 60 H, Germany) operating at a fixed frequency of 37 KHz ultrasonic irradiation with 150 W of ultrasonic power was used for this experiment. The temperature of suspension was kept constant at $25 \pm 3°C$ by adding ice cubes in the bath water. During the sonocatalytic degradation experiment, samples of about 3 mL were withdrawn periodically from the vessel. After filtration through Milipore (0.22 μm, PVDF) of syringe filter, the filtrate was then determined the absorbance of remaining AO7 solution by using Lambda 25 UV-VIS Spectrophotometer (Perkin Elmer, USA).

In this study, experiment of sonolysis system (without catalyst: US) was also carried out and the results were then compared with the sonocatalytic system (with catalysts: US + ZnO and US + Fe_2O_3/ZnO). The attention is to assess the role of catalysts under ultrasonic reaction. Besides, the sonocatalytic system for both catalysts, ZnO and Fe_2O_3/ZnO, had been run in order to identify the effect of Fe_2O_3 particles loading on the surface of ZnO particles and sonocatalytic activity between these two catalysts.

To establish a calibration curve between sample absorbance and concentration, a standard AO7 solutions with a concentration from 4 to 20 mg/L were prepared and analyzed at a maximum wavelength of 484 nm. In order to determine the change in the molecular structure of AO7 (Figure 2), the wavelength of this solution was scanned from 350 nm to 600 nm.
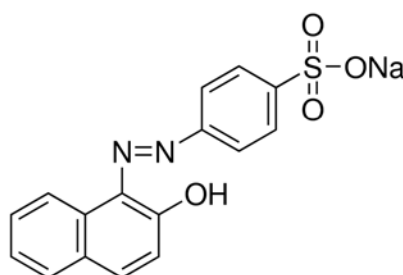

Figure 2: Chemical structure of Acid Orange 7

An equation of linear relationship between absorbance and concentration was obtained from the standard AO7 solutions. Then, the concentrations of samples were determined based on the established equation. Meanwhile, the performance of removal for AO7 solution was calculated by using the following equation:

Removal of AO7 solution (%) = $(C_i - C/ C_i)$ x 100

where C_i is the initial concentration of AO7 solution (adsorption–desorption equilibrium) and C is the final concentration of AO7 solution after a certain irradiation time (min).

3. RESULTS AND DISCUSSIONS

3.1 Structural, Surface Area, Elemental and Morphological Analyses of ZnO and Fe_2O_3/ZnO

The presence of Fe_2O_3 particles loading on the surface of ZnO particles was confirmed by comparing the XRD pattern of ZnO catalyst and Fe_2O_3/ZnO composite catalyst. These two patterns are shown in Figure 3 (a) for ZnO catalyst and Figure 3 (b) for Fe_2O_3/ZnO composite catalyst. Both samples have a diffraction peak at 34.42° or so which corresponded to the diffraction of (002) plane of wurzite-structured ZnO (PDF No. 00-036-1451) [14]. Composite catalyst of Fe_2O_3/ZnO demonstrated the weaker (002) peak (Figure 3 (b)) and smaller FWHM compared to ZnO catalyst (Table 1). However, the crystallite size of Fe_2O_3/ZnO composite catalyst was slightly larger than ZnO catalyst. It indicates that the crystalline quality of ZnO particles was weakened when Fe_2O_3 particles were loaded on the surface of ZnO particles. The loading of Fe_2O_3 particles influenced the crystalline quality and growth orientation which might be due to the preparation techniques applied and starting materials used.

XRD result also revealed that both catalysts have shown an identical major peaks present in the spectra. The characteristic peaks of ZnO were seen at 2θ values of 31.85° (100), 34.49° (002), 36.35° (101), 47.55° (102), 56.66° (110) and 62.88° (103). Meanwhile the peaks for Fe_2O_3 can be observed at 2θ values of 31.81° (100), 34.42° (002), 36.24° (101), 47.59° (102), 56.57° (110) and 62.87° (103) in composite catalyst. However, the intensities for all the identical peaks were decreased significantly for Fe_2O_3/ZnO as the composite catalyst. This might be due to the influence of Fe_2O_3 loading which affected the crystalline quality and growth orientation as discussed earlier.
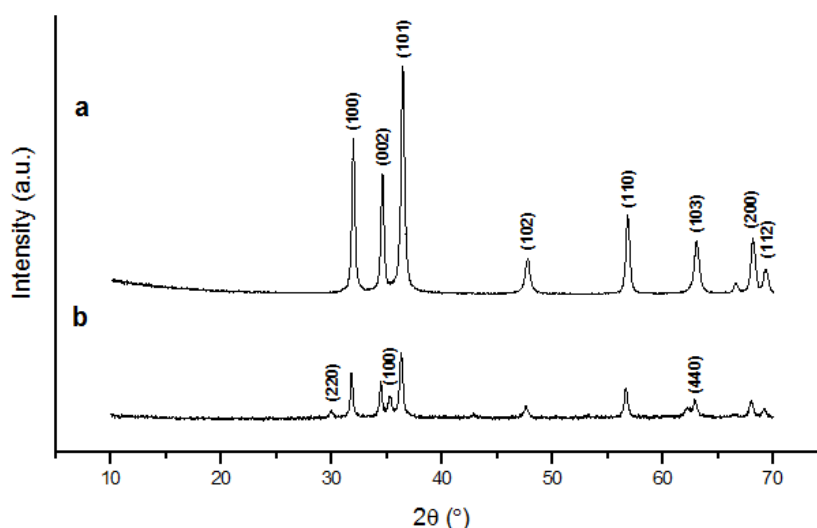

Figure 3: XRD pattern (a) ZnO catalyst (b) and Fe_2O_3/ZnO composite catalyst

For composite catalyst, another three peaks at 29.94° (220), 35.34° (100) and 62.88° (440) were also observed besides the identical peaks which attributed to the loaded Fe_2O_3 particles on the surface of ZnO particles (PDF 00-004-0755). From the above data, it can be demonstrated that the loading of Fe_2O_3 particles on the surface of ZnO particles led to the spectra peak which were shifted slightly to the left (smaller 2θ) for most of the peaks. This small shifting peak (refer to (002) peak [14]), indicating that the lattice strain of Fe_2O_3/ZnO particles was relatively too small compared to ZnO particles. Therefore, there was no significant change in crystallite size of Fe_2O_3/ZnO particles as can be seen in Table 1.

Table 1: XRD data of ZnO catalyst and Fe_2O_3/ZnO composite catalyst

Catalyst	FWHM	Lattice strain	Average crystallite size (nm)
ZnO	0.35415	0.0047	24.69
Fe_2O_3/ZnO	0.31260	0.0042	27.94

Table 2 lists the surface area, pore volume and pore size for ZnO catalyst and Fe_2O_3/ZnO composite catalyst. From this table, both samples demonstrated a mesoporous structure with the pore sizes of ZnO catalyst and Fe_2O_3/ZnO composite catalyst to be at 22.92 and 5.309 nm, respectively. Besides, N_2 gas absorption-desorption isotherms for both catalysts exhibited the Type IV category. This result supports the pore size data which the as-prepared catalyst and composited catalyst are mesoporous material [15]. On the other hand, Fe_2O_3/ZnO composite catalyst demonstrated a significant surface area and pore volume increment which were ~6.7 and ~1.5 relatively higher compared to ZnO catalyst due to the loading of Fe_2O_3 particles on its surface.

Table 2: Structure properties of ZnO catalyst and Fe_2O_3/ZnO composite catalyst

Catalyst	Surface Area (m²/g)	Pores Volume (cm³/g)	Pores size (nm)
ZnO	17.21	0.0986	22.92
Fe_2O_3/ZnO	116.11	0.1541	5.309

EDX results show that zinc and oxygen atoms and zinc, oxygen and iron atoms are in the as-prepared catalysts (Figure 4). Surface composition in terms of atomic % for ZnO catalyst was 43.6% Zn and 35.6% O and for Fe_2O_3/ZnO composite catalyst was 48.1% Zn, 18.8% O and 10.2% Fe. This result confirmed the formation of ZnO and Fe_2O_3/ZnO, and it also indicates that the loading Fe_2O_3/ZnO particles on the surface of ZnO particles was successfully achieved. Meanwhile, it is noteworthy that the carbon atom peak in the EDX spectra originated from a carbon adhesive tape.
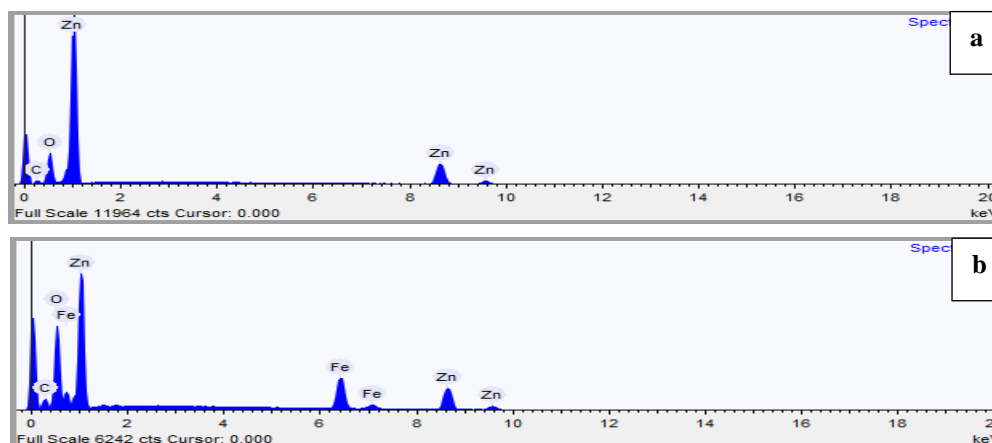
Figure 4: EDX spectrum (a) ZnO catalyst (b) and Fe_2O_3/ZnO composite catalyst

Surface morphologies of ZnO catalyst and Fe_2O_3/ZnO composite catalyst are shown in Figure 5. The surface morphology characteristic for both catalysts are almost similar whereby the loading of Fe_2O_3 particles on the surface of ZnO particles could not obviously be observed or distinguished as shown in SEM images. This finding was supported by XRD (Table 1) analysis as discussed in the earlier section, by which both catalysts have exhibited only a small difference in terms of their relative crystallite sizes. Besides, both ZnO catalyst and Fe_2O_3/ZnO composite catalyst possessed an irregularity in shape and size which can contribute to the growth of non-uniform crystalline grains during the synthesis [16]. Visually, the needle-like shape crystals that attributed to ZnO particles can be noticed to be evenly dispersed as depicted from the SEM image (Figure 5 (b)) [17]. Moreover, the SEM image also revealed that the presence of Fe_2O_3 particles on the surface of ZnO particles did not change the quality of the agglomeration particles.

3.2 Sonolytic (US) and Sonocatalytic (US + ZnO and US + Fe_2O_3/ZnO) Degradations of AO7 Solution

Figure 6 shows removal (%) of AO7 solution for three systems which are (1) sonolysis (US); (2) sonocatalysis (US + ZnO catalyst) and (3) sonocatalysis (US + Fe_2O_3/ZnO composite catalyst). At 0 minute (after adsorption–desorption activity), both catalysts have shown an adsorption activity especially Fe_2O_3/ZnO composite catalyst due to the significant removal of AO7 solution at 72.7%, as compared to ZnO catalyst which was only 17.4%. This result demonstrates that the performance of Fe_2O_3/ZnO composite catalyst was better than ZnO catalyst in this activity due to high amount of AO7 molecules adsorbed on the catalyst particles which were influenced by the high quality of its physical properties such as the surface area. This result is in good agreement with the surface area of Fe_2O_3/ZnO composite catalyst as discussed in Subsection 3.1.
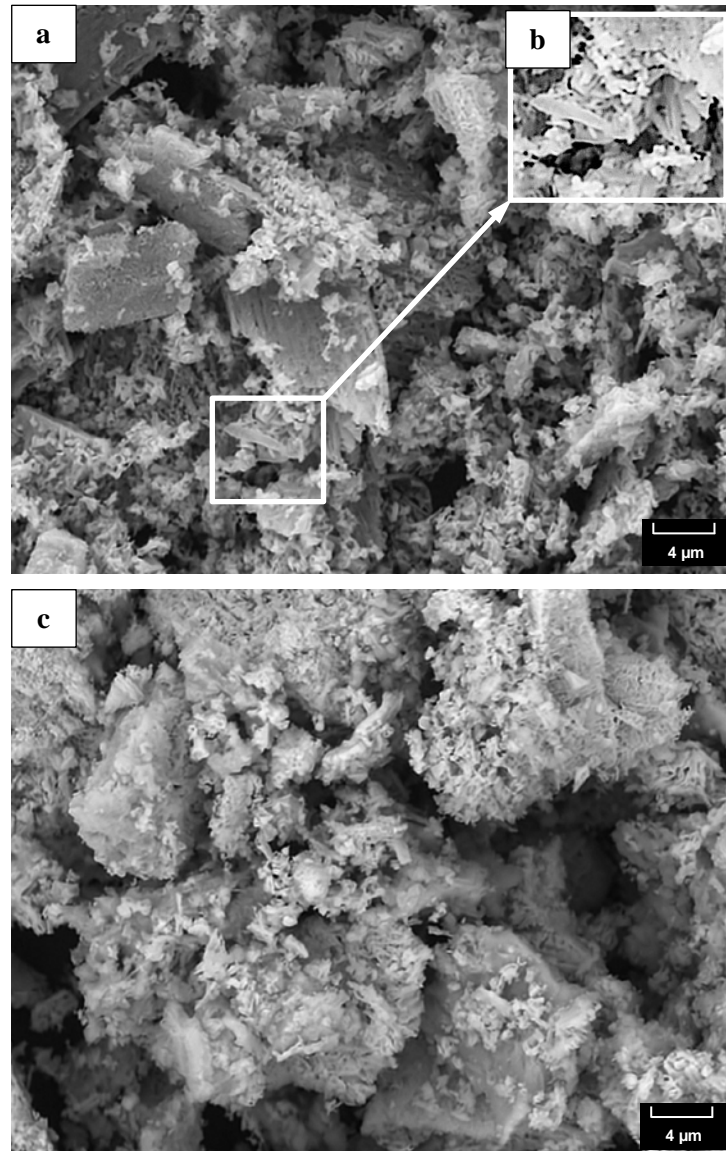
Figure 5: SEM images of ZnO (a) and Fe$_2$O$_3$/ZnO (b)

However, sonocatalytic system (both catalysts) displayed the removal of AO7 solution in less than 10% throughout the preferable time indicating that the performance of sonocatalytic activity for both catalysts exhibiting insignificant removal of AO7 solution. This result demonstrates that the sonocatalytic system was mostly not contributed by catalytic activity. This finding could be confirmed by comparing the removal pattern of AO7 solution for sonolytic system (average removal is less than ~7%).A possible reason for this finding is due to only a trace amount of •OH radicals that were generated on the irradiated surface of both catalysts under the ultrasonic condition. Thus, this indicates that the as-prepared catalysts (ZnO and Fe$_2$O$_3$/ZnO) with the applied parameter conditions were unable to promote sufficient oxidation of AO7 solution. The sonocatalytic degradation efficiency was obviously affected by ultrasonic irradiation time, solution acidity, initial concentration and reaction temperature [8]. The detail of the result findings can be further discussed by referring to the next figure.

The result in term of spectral change of AO7 solution before and after ultrasonic radiation is shown in Figure 7. The changes of peak at $\lambda_{max} = 484$ nm was chosen for monitoring of the AO7 solution removal. The peak intensity (absorbance) slightly decreased from 0 min to 120 min for all three systems (US, US + ZnO and US + Fe$_2$O$_3$/ZnO). This result also exhibits almost no change in the matter of spectra pattern. Besides, there was no wavelength shift of the spectra for all systems between the interval times. This indicates that there is no positive catalytic role of ZnO catalyst and Fe$_2$O$_3$/ZnO composite catalyst under ultrasonic radiation at the parameter condition. The result was probably due to only a trace amount of •OH radicals or nearly no •OH radicals were generated by the ultrasonic cavitation at this parameter condition. It indicates that there was no catalytic activity during the sonocatalytic experiments. Therefore, this finding is parallel with the result of removal product which AO7 molecule has the same compound after the ultrasonic irradiation.
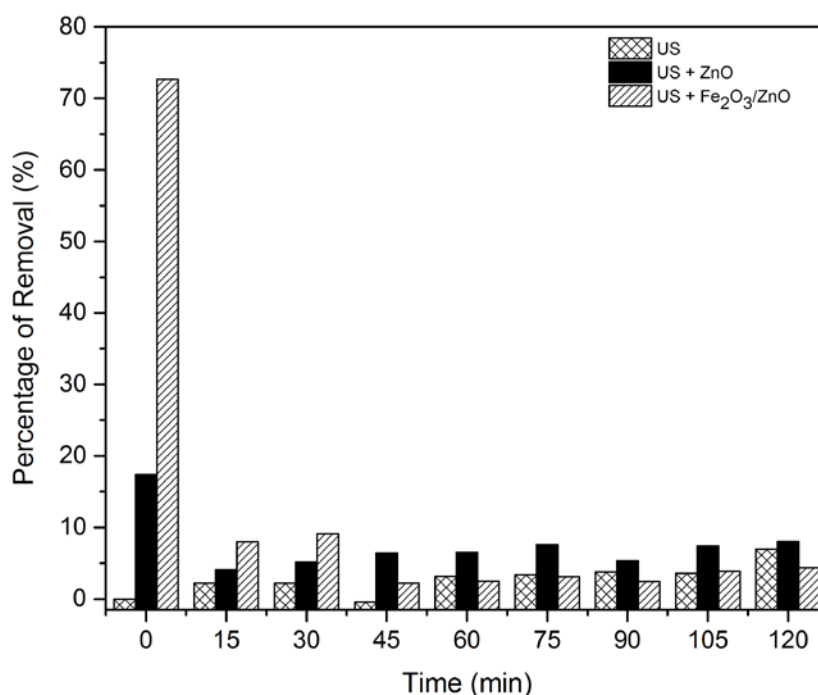

Figure 6: Removal (%) of AO7 solution for sonolysis and sonocatalysis
(Three different systems: (1) US, (2) US + ZnO and (3) US + Fe$_2$O$_3$/ZnO)
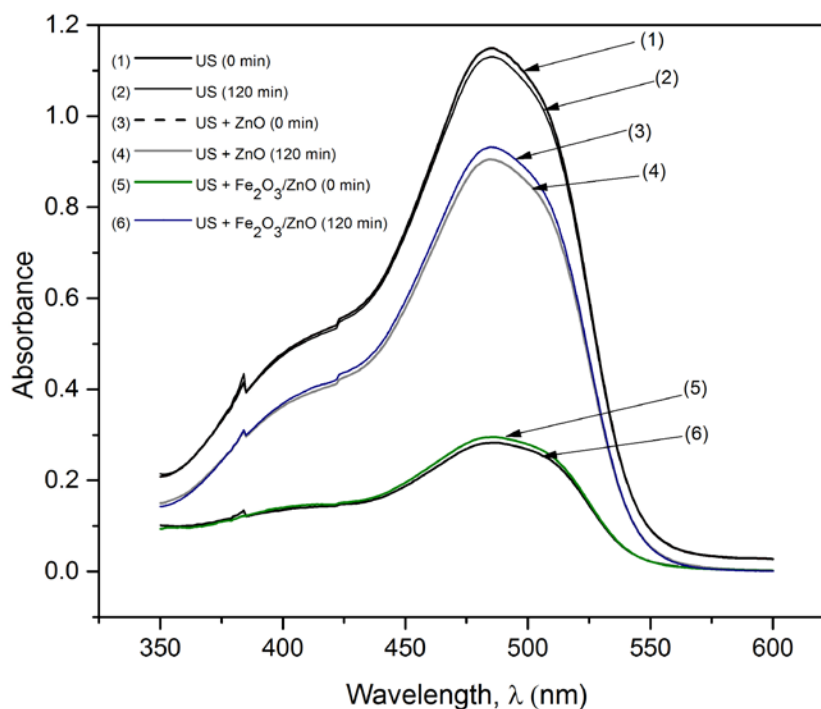
Figure 7: UV/vis absorbance spectra of AO7 solution before and after ultrasonic radiation (Three different systems: (1) US, (2) US + ZnO and (3) US + Fe_2O_3/ZnO)

4. CONCLUSION

In summary, the synthesized of Fe_2O_3/ZnO composite catalyst via a sol-gel/precipitation method was successfully prepared based on the characterization results. Structural and elemental analyses revealed that the Fe_2O_3 particles loaded on ZnO particles and this loading resulted in high surface area compared to ZnO catalyst. However, the poor removal of AO7 solution in sonocatalytic experiment using this composite catalyst indicated that this catalyst was not a good potential as a sonocatalyst in the treatment of azo dyes. This may be due to only a trace amount of •OH radicals or nearly no •OH radicals that were generated by the ultrasonic cavitation at this parameter condition. In addition, this study has revealed that Fe_2O_3/ZnO composite catalyst was superior to the adsorption activity in removing of AO7 from aqueous solution due to adsorption ability of Fe_2O_3.

REFERENCES

[1]   M. Muruganandham and M. Swaminathan, "Solar photocatalytic degradation of a reactive azo dye in TiO_2-suspension," *Sol. Energy Mater. Sol. Cells*, vol. 81 (4), pp. 439–457, 2004.

[2]   S. Yang, P. Wang, X. Yang, L. Shan, W. Zhang, X. Shao, and R. Niu, "Degradation efficiencies of azo dye Acid Orange 7 by the interaction of heat, UV and anions with common oxidants: Persulfate, peroxymonosulfate and hydrogen peroxide," *J. Hazard. Mater.*, vol. 179 (1–3), pp. 552–558, 2010.

[3] M. Jagannathan, F. Grieser, and M. Ashokkumar, "Sonophotocatalytic degradation of paracetamol using TiO_2 and Fe^{3+}," *Sep. Purif. Technol.*, vol. 103, pp. 114–118, 2013.

[4] Y. Areerob, C. J. Yong, J. W. Kweon, and W.-C. Oh, "Enhanced sonocatalytic degradation of organic dyes from aqueous solutions by novel synthesis of mesoporous Fe_3O_4-graphene/$ZnO@SiO_2$ nanocomposites," *Ultrason. Sonochem.*, 2017.

[5] L. Song, C. Chen, S. Zhang, and Q. Wei, "Sonocatalytic degradation of amaranth catalyzed by La^{3+} doped TiO_2 under ultrasonic irradiation," *Ultrason. Sonochem.*, vol. 18 (5), pp. 1057–1061, 2011.

[6] Y. Zhai, Y. Li, J. Wang, J. Wang, L. Yin, Y. Kong, G. Han, and P. Fan, "Effective sonocatalytic degradation of organic dyes by using Er^{3+}:$YAlO_3$/TiO_2–SnO_2 under ultrasonic irradiation," *J. Mol. Catal. A Chem.*, vol. 366, pp. 282–287, 2013.

[7] A. R. Khataee, A. Karimi, R. D. C. Soltani, M. Safarpour, Y. Hanifehpour, and S. W. Joo, "Europium-doped ZnO as a visible light responsive nanocatalyst: Sonochemical synthesis, characterization and response surface modeling of photocatalytic process," *Appl. Catal. A Gen.*, vol. 488, pp. 160–170, 2014.

[8] J. Wang, Z. Jiang, L. Zhang, P. Kang, Y. Xie, Y. Lv, R. Xu, and X. Zhang, "Sonocatalytic degradation of some dyestuffs and comparison of catalytic activities of nano-sized TiO_2, nano-sized ZnO and composite TiO_2/ZnO powders under ultrasonic irradiation," *Ultrason. Sonochem.*, vol. 16 (2), pp. 225–231, 2009.

[9] R. K. Sharma and R. Ghose, "Synthesis of Co_3O_4-ZnO mixed metal oxide nanoparticles by homogeneous precipitation method," *J. Alloys Compd.*, vol. 686 (3), pp. 64–73, 2016.

[10] J. Lang, J. Wang, Q. Zhang, X. Li, Q. Han, M. Wei, Y. Sui, D. Wang, and J. Yang, "Chemical precipitation synthesis and significant enhancement in photocatalytic activity of Ce-doped ZnO nanoparticles," *Ceram. Int.*, vol. 42 (12), pp. 14175–14181, 2016.

[11] Z. Zhou, W. Li, J. Song, G. Yi, B. Mei, and L. Su, "Synthesis and characterization of Nd^{3+} doped SrF_2 nanoparticles prepared by precipitation method," *Ceram. Int.*, no. April, pp. 0–1, 2017.

[12] L. Znaidi, T. Chauveau, A. Tallaire, F. Liu, M. Rahmani, V. Bockelee, D. Vrel, and P. Doppelt, "Textured ZnO thin films by sol–gel process: Synthesis and characterizations," *Thin Solid Films*, vol. 617, pp. 156–160, 2016.

[13] X. Su, Y. Jia, X. Liu, J. Wang, J. Xu, X. He, C. Fu, and S. Liu, "Preparation, dielectric property and infrared emissivity of Fe-doped ZnO powder by coprecipitation method at various reaction time," *Ceram. Int.*, vol. 40 (4), pp. 5307–5311, 2014.

[14] L. Xu and X. Li, "Influence of Fe-doping on the structural and optical properties of ZnO thin films prepared by sol-gel method," *J. Cryst. Growth*, vol. 312 (6), pp. 851–855, 2010.

[15] K. W. Kolasinski, *Surface Science*. Chichester, UK: John Wiley & Sons, Ltd, 2012.

[16] A. Khataee, S. Saadi, B. Vahid, S. W. Joo, and B. K. Min, "Sonocatalytic degradation of Acid Blue 92 using sonochemically prepared samarium doped zinc oxide nanostructures," *Ultrason. Sonochem.*, vol. 29, pp. 27–38, 2016.

[17] J. Xu, Y. Chang, Y. Zhang, S. Ma, Y. Qu, and C. Xu, "Effect of silver ions on the structure of ZnO and photocatalytic performance of Ag/ZnO composites," *Appl. Surf. Sci.*, vol. 255 (5) part 1, pp. 1996–1999, 2008.